Journal of Chemical, Biological and Physical Sciences

An International Peer Review E-3 Journal of Sciences

*Available online at*www.jcbsc.org

Section C: Physical Sciences

CODEN (USA): JCBPAT Research Article

Effect of Vanadium Doping on Structural Properties of SnO_2 Thin Films Prepared by Chemical Spray Pyrolysis Method

Ziad T. Khodair[1], Nabeel A. Bakr[1*], Adnan A. Mohammed[1, 2]

[1]Department of Physics, College of Science, University of Diyala, Diyala, Iraq.

[2]Diyala General Directorate of Education, Diyala, Iraq.

Received: 11 November 2015**; Revised:** 23 November 2015; **Accepted:** 04 December 2015

Abstract: In this study, ($Sn_{1-x}V_xO_2$) thin films, where (x = 0, 4, 6 and 8) % have been deposited on glass substrates by chemical spray pyrolysis technique (CSP) at substrate temperature of (400 $^{\circ}$C) and thickness of about 400 ± 10 nm. The structural properties and morphology of these films have been studied using XRD and AFM respectively. XRD analyses showed that these films are polycrystalline in nature with tetragonal Rutile structure with preferred orientation of (110). Doping with Vanadium causes decrease in the grain size and increase in dislocation density, micro strain, and interplanar spacing.

Keywords: SnO_2 thin films, Vanadium Doping, Chemical Spray Pyrolysis, Structural Properties.

INTRODUCTION

Tin dioxide (SnO_2), is an important n-type semiconductor with tetragonal Rutile structure having lattice parameters a = b = 4.737 Å and c = 3.826 Å. The unit cell contains two tin and four oxygen atoms. Each tin atom is bounded to six oxygen atoms at the corners of a regular octahedron, and every oxygen atom is surrounded by three tin atoms[1]. Tin oxide has been extensively investigated for gas sensors, optical-conductive coatings for solar cells and electrocatalytic anodes[2,3], glass coatings for furnace windows as well as transparent electrodes for liquid crystal displays[4]. Tin dioxide (SnO_2) has a density of (6.95 g/cm^3) and molecular weight of (150.69 g/mol). Its melting point is (2643 K)[5]. SnO2 films have been fabricated using various technologies such as sol-gel, spray pyrolysis, ion beam sputtering, magnetic sputtering, and pulsed laser[6]. Vanadium (V) lies with the transition metals on the

periodic table. The atomic number of Vanadium is 23 with an atomic mass of 50.94 amu[7]. In this study we report the effect of (V) doping on the structural properties of SnO_2 film.

EXPERIMENTAL PROCEDURE

Chemical spray pyrolysis technique was used to deposit undoped and V-doped (SnO_2) films on glass substrates at temperature of (400 ºC). A homogeneous solution was prepared by dissolving ($SnCl_4.5H_2O$) and (VCl_3) powders in distilled water at the concentration of 0.1 M at room temperature in which the volumetric ratios of V were (0, 2, 4, 6 and 8) %. The resultant solution was sprayed on glass substrate. Other deposition conditions such as spray nozzle substrate distance (30 cm), spray time (7 s), spray interval (3 min) and pressure of the carrier gas (1.5 bar) were kept. The X-ray diffraction patterns for the prepared films were obtained in a (Shimadzu XRD-6000) goniometer using copper target (CuKα, 1.5416 Å) and Atomic Force Microscopy (AFM) micrographs were recorded by using scanning probe microscope type (SPM- AA3000), contact mode, supplied by Angstrom Advanced Inc.

RESULTS AND DISCUSION

Structural analysis: The X-ray diffraction patterns of undoped and V doped SnO_2 deposited at 400 ^oC are shown in Figure (1). The highest three diffraction peaks are (110), (101) and (200), which is in agreement with the International Centre for Diffraction Data (ICDD) card number (41-1445) with a tetragonal unit cell showing a preferred orientation along (110). V doping led to a decrease in the intensity of the diffraction peaks.

The average crystallite size: The average crystallite size for the films can be determined using Williamson-Hall formula shown below[8]:

$$\beta_{hk\ell}\cos\theta = \left(\frac{K\lambda}{D}\right) + 4S\sin\theta \qquad (1)$$

Where βhkl is full width of half maximum, D is the average crystallite size, k is constant and was assumed to be equal to 0.9, λ is wavelength for Cu target for XRD instrument, θ is Bragg's angle for all peaks, and S is the microstrain in the film. If βcosθ is plotted with respect to 4sinθ for all peaks, strain and crystallite size can be calculated from the slope and y-intercept of the fitted line respectively as shown in Figure (2). The average crystallite size for the all films is also calculated for (110) direction by Scherrer's formula by using the relation[9]:

$$D = K\lambda / \beta \cos\Theta \qquad (2)$$

It is observed that the crystallite size of Tin Oxide thin films from the (110) peaks decreases when ratio of doping by V increases. The values of average crystallite size are in the range of (2.68 - 4.54) nm as shown in Figure (2). The decrease in average crystallite size shows that at least a small quantity of V4+ ions substituted the Sn ions, since the V4+ ionic radius (0.58 Å) is smaller than that corresponding to Sn4+ ion (0.71 Å)[10]. These results agree qualitatively with the results of crystallite size obtained by Williamson-Hall method as shown in **Table (1)**. The microstrain in the films is induced during the growth of thin films by varying displacements of the atoms with respect to their reference lattice position[11]. All values of microstrain were negative which indicates the occurrence of compression in the lattice, as shown in **Table (1)**.

Table 1: Structural parameters of V-doped Tin Oxide thin films.

Sample		Undoped SnO_2	$Sn_{0.98}V_{0.02}O_2$	$Sn_{0.96}V_{0.04}O_2$	$Sn_{0.94}V_{0.06}O_2$	$Sn_{0.92}V_{0.08}O_2$
hkl		1 1 0	1 1 0	1 1 0	1 1 0	1 1 0
2θ (deg)		26.3686	26.5284	26.5284	26.3287	26.7879
d_{hkl} (Å)		3.3770	3.35728	3.35728	3.38229	3.32534
FWHM (deg)		1.80	2.05	2.32	2.78	3.05
D_{av} (nm)	Scherrer	4.54	3.98	3.52	2.94	2.68
	W-Hall	3.9	3.37	2. 6	2.1	1.87
δ (nm^{-2})	Scherrer	0.0485	0.0631	0.0807	0.1156	0.1392
	W-Hall	0.0657	0.0730	0.1957	0.2267	0.2859
N_o (nm^{-2})	Scherrer	4.2745	6.2344	9.1232	15.7404	20.7804
	W-Hall	6.7432	10.4512	34.6525	43.1918	61.1695
$T_{c(hkl)}$		1.6949	1.7964	1.8072	1.7241	1.6666
Microstrain $S*10^{-3}$		-8.15	-27.08	-34.93	-38.4	-41.59
Lattice constant a_o (Å)		4.7761	4.74791	4.74791	4.78328	4.70274
Lattice constant c_o Å		3.1672	3.1542	3.1542	3.2053	3.1908

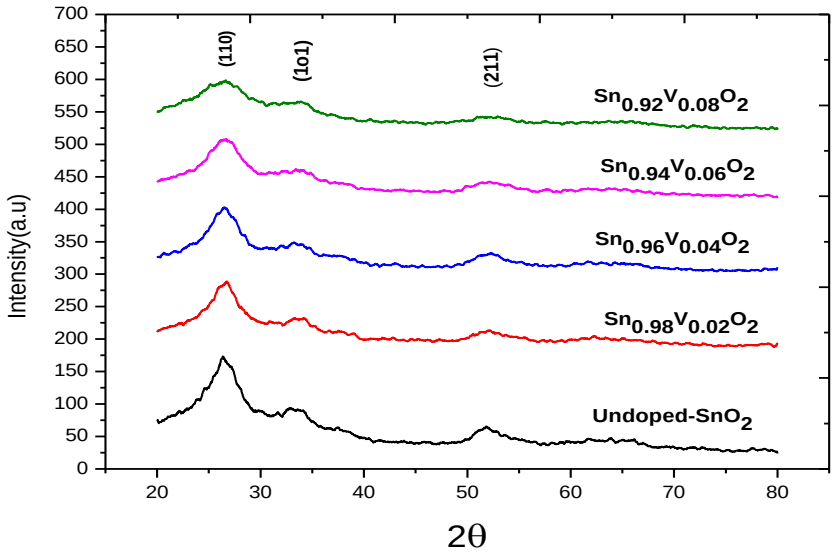

Fig. 1: X-ray diffraction pattern of the undoped and V doped SnO_2.

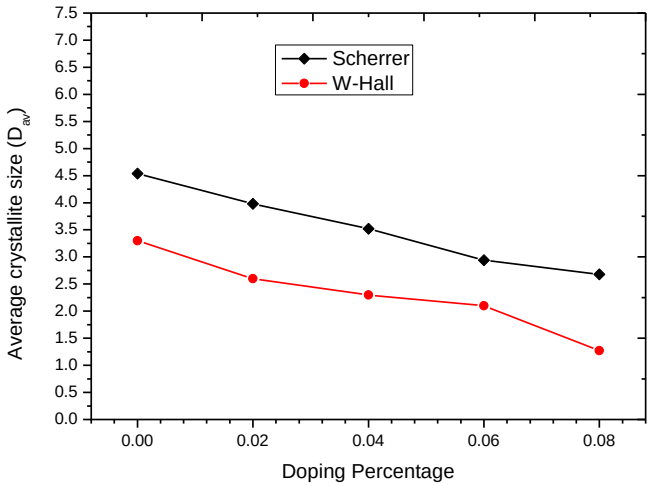

Fig. 2: Average crystallite size as a function of doping percentage.

Texture coefficient $T_c(hkl)$: The texture coefficient (*Tc*) represents the texture of a particular plane, in which greater than unity values imply that there are numerous of grains in that particular direction. The texture coefficients *Tc(hkl)* for all samples have been calculated from the X-ray data using the well-known formula[12]:

$$T_C(hkl) = \frac{I(hkl)/I_0(hkl)}{N_r^{-1}\sum I(hkl)/I_0(hkl)} \quad (3)$$

Where *I(hkl)* is the measured intensity, $I_o(hkl)$ taken from the ICDD standard data, (Nr) is the number of peaks and *(hkl)* are Miller indices. The texture coefficient is calculated for crystal plane (110) of the undoped and V- doped SnO_2 films. All values of texture coefficient were greater than 1 which indicates the abundance of grains in the (110) direction.

Specific Surface Area (SSA): SSA is the area per unit mass. It is very important factor in the field of nanoparticles because of large surface to volume ratio of such small particle size materials[13,14]. SSA used in materials to determine their types and properties and is also used in case of reactions on surfaces, heterogeneous catalysis and adsorption[15]. Mathematically, SSA can be determined by using the following relation[16]:

$$SSA = 6 * 10^3 / D.\ \rho \quad (4)$$

Where, SSA is the specific surface area and ρ is the density of undoped and V doped SnO_2. The values of the Specific surface area of all the deposited samples are shown in table (2). It is clear that SSA increases as the particle size decreases.

(AFM) Result: The 3D AFM micrographs of the undoped and V doped SnO_2 thin films are shown in Figure (4). The size of the scanned area was (2×2) μm^2. AFM results show homogenous and smooth thin films. The average grain size, average roughness and root mean square (RMS) roughness for all samples estimated from AFM are given in **Table (3)**. The average grain size, average roughness and RMS roughness of the film decrease when ratio of doping by V increases for all samples except the ratio of 6% where the particle size increases. The results of grain size obtained from AFM investigation are qualitatively in agreement with those obtained from XRD analysis shown in **Table (2).**

Table 2: Specific surface area of undoped and V doped SnO_2.

Sample	ρ ($g.cm^{-3}$)	D_{av} (nm)		SSA ($m^2.g^{-1}$)	
		Scrherer	W-Hall	Scherrer	W-Hall
Undoped- SnO_2	6.95	4.54	3.9	188	221
$Sn_{0.98}V_{0.02}O$	6.87814	3.98	3.37	219	259
$Sn_{0.96}V_{0.04}O$	6.80628	3.52	2.6	250	339
$Sn_{0.94}V_{0.06}O$	6.73442	2.94	2.1	303	424
$Sn_{0.92}V_{0.08}O$	6.66256	2.68	1.87	336	481

Table 3: The crystallite size of undoped and V doped SnO_2 thin films.

Sample	Surface roughness (nm)	RMS (nm)	Grain size (nm)
Undoped- SnO_2	4.7	8.61	98.68
$Sn_{0.98}V_{0.02}O_2$	2.68	3.24	98.05
$Sn_{0.96}V_{0.04}O_2$	2.47	2.93	95.21
$Sn_{0.94}V_{0.06}O_2$	2.82	3.29	100.79
$Sn_{0.92}V_{0.08}O_2$	6.05	6.95	87.9

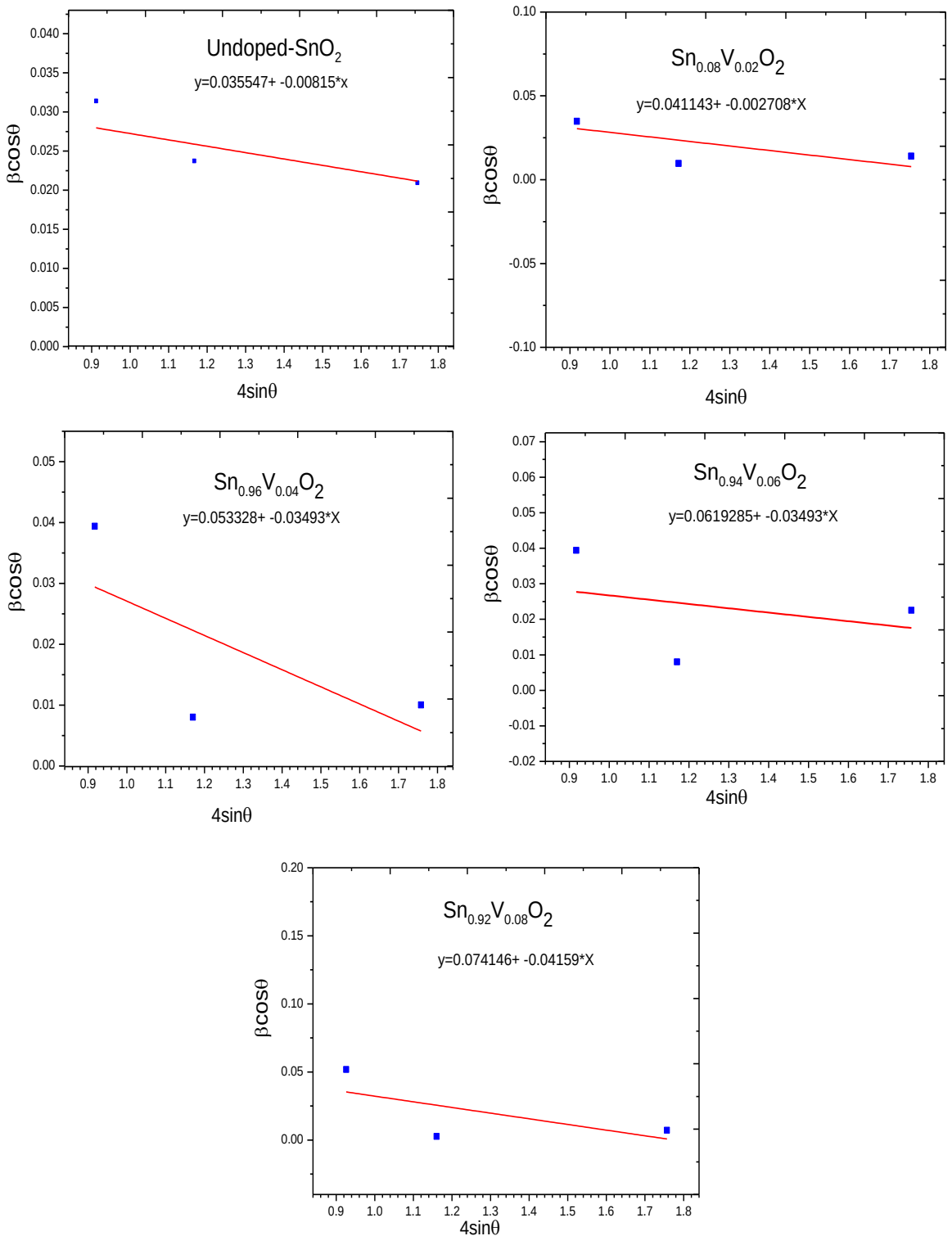

Fig. 3: W-H analysis of V-doped Tin Oxide thin films

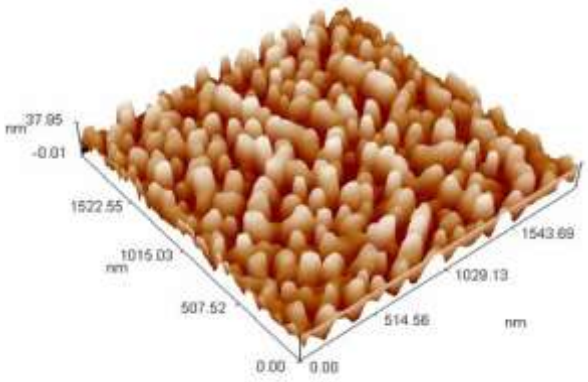

Undoped Sn_2O_2

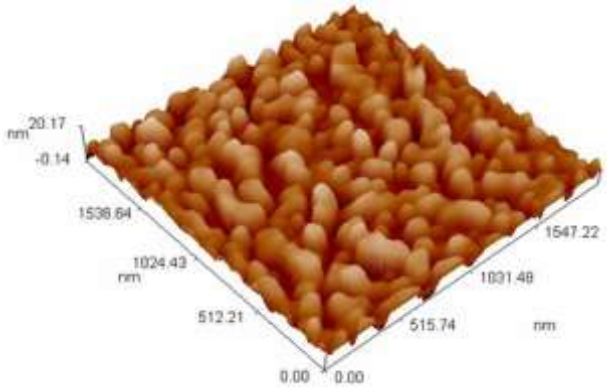

$Sn_{0.98}V_{0.02}O_2$

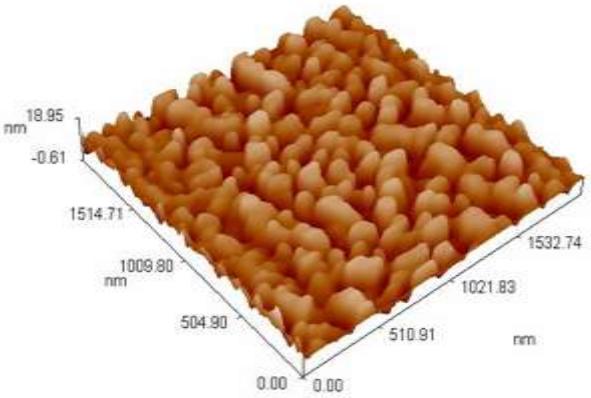

$Sn_{0.94}V_{0.02}O_2$

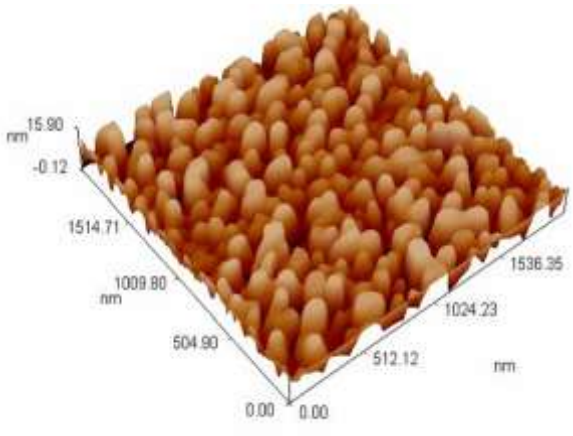

$Sn_{096}V_{0.04}O_2$

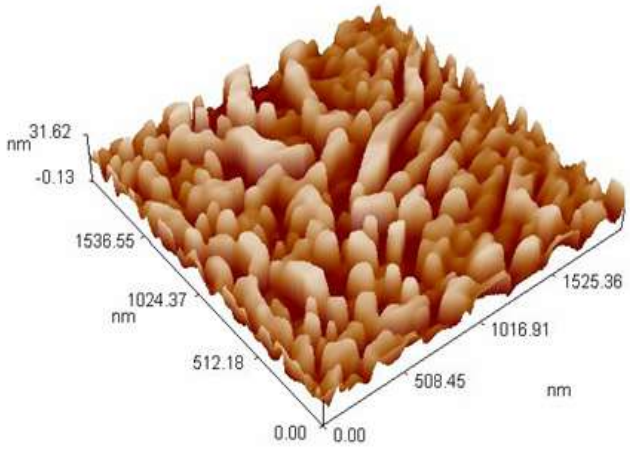

$Sn_{0.92}V_{0.08}O_2$

Fig. 4: 3D AFM images of undoped and V doped SnO_2 thin films.

CONCLUSIONS

Thin films of $Sn_{1\_x}V_xO_2$, where x = 0, 0.02, 0.04, 0.06 and 0.08 have been successfully synthesized by chemical spray pyrolysis technique. The Influence of doping on structural and morphological properties of these films was investigated. The XRD results showed that all films are polycrystalline in nature with tetragonal structure and preferred orientation along (110) plane. The intensity of peaks, the crystallite size and lattice constants decreased with increasing of doping, while dislocation density, number of crystal and Specific Surface Area increased with increasing of doping. AFM results showed that the average grain size, average roughness and root mean square (RMS) decreased with increasing of doping. These results were qualitatively in agreement with the results of crystallite size obtained by XRD results.

REFERENCES

1. C. Wang, X. Chu and M. Wu, Highly sensitive gas sensors based on hollow SnO_2 spheres prepared by carbon sphere template method, *Sensors and Actuators B*, 2007, 120, 508-513.
2. S. C. Ray, M. K. Karanjai and D. Dasgupta, Tin dioxide based transparent semiconducting films deposited by the dip-coating technique, *Surface and Coatings Technol*., 1989, 102(1), 73-80.
3. L. A. Patil**,** Ultrasonically sprayed nanostructured SnO_2 thin films for highly sensitive hydrogen sensing, ISBN 978-1-4398-34015, 2010, 1.
4. A. J. Freeman, K. R. Poeppelmeier, T. O. Mason, R. P. H. Chang and T. J. Marks, Chemical and thin-film strategies for new transparent conducting oxides, *MRS Bull.*, 2000, 25, 45-51.
5. J. E. House and K. A. House, Descriptive Inorganic Chemistry, Illinois Wesleyan University, Bloomington, Illinois, 2010.
6. K. L. Chopra and I. Kaur, Thin Film Device Applications, Plenum press, New York, 1983.
7. R. R. Moskalyk and A. M. Alfantazi, Processing of vanadium: a review, *Minerals Engineering*, 2003, 16, 793–805.
8. Y. T. Prabhu, K. V. Rao, V. S. Kumar and B. S. Kumari, X-Ray Analysis by Williamson-Hall and Size-Strain Plot Methods of ZnO Nanoparticles with Fuel Variation, *World Journal of Nano Science and Engineering*, 2014, 4, 21-28.
9. R. H. Bari and S. B. Patil, Studies on spray pyrolised nanostructured SnO_2 thin films for H_2 gas sensing application, *International Letters of Chemistry, Physics and Astronomy*, 2014, 17(2), 125-141.
10. A. Popa, D. Toloman, O. Raita, M. Stan and O. Pana, Ferromagnetic Behavior of Vanadium Doped SnO_2 Nanoparticles annealed at Different Temperatures, *Journal of Alloys and Compounds*, 2014, 591, 201-206.
11. N. A. Bakr, Z. T. Khodair and A. M. Shano, Effect of Aqueous Solution Molarity on Structural and Optical Properties of $Ni_{0.92}Co_{0.08}O$ Thin Films Prepared by Chemical Spray Pyrolysis Method, *Int. J. Thin. Fil. Sci. Tec.*, 2015, 4(2), 111-119.
12. C. Barret and B. T. Massalki, Structure of Metals, Oxford, Pergamon, 1980.
13. M. E. Nielsen and M. R. Fisk, Data report: Specific surface area and physical properties of subsurface basalt samples from the east flank of Juan de Fuca Ridge, Proceedings of the Integrated Ocean Drilling Program, 2008, 301.

14. A. Rahdar, V. Arbabi and H. Ghanbari, Study of electro-optical properties of ZnS nanoparticles prepared by colloidal particles method, *International Journal of Chemical and Biological Engineering*, 2012, 6, 550-552.
15. T. Theivasanthi and M. Alagar, Konjac biomolecules assisted–rod/ spherical shaped lead nano powder synthesized by electrolytic process and its characterization studies, *Nano Biomed. Eng.*, 2013, 5, 11-19.
16. T. Theivasanthi and M. Alagar, Electrolytic synthesis and characterization of silver nanopowder, *Nano Biomed. Eng.*, 2012, 4, 58-65.

*** Corresponding author: Nabeel A. Bakr;**

1\Department of Physics, College of Science, University of Diyala, Diyala, Iraq.